

Forest fire disaster risk analysis using Sentinel 2 and Landsat images case study: Al-Qoubaiyat and Tyre regions, Lebanon

Mohamed Issa*¹, Mohammad Abboud¹

¹Lebanese International University, School of Engineering, Topographic Surveying Department, Beirut, Lebanon

Keywords

DRR
Forest Fire
Satellite Remote Sensing
Burn Index
GIS
Lebanon

ABSTRACT

Fires are considered a threat to the world with all its components and sectors. Recently, it is noticeable an increase in these fires that hit many countries, especially in Lebanon which is considered a country, rich in forests. A forest fire can be naturally caused by either global warming or high temperature. On the other hand, it may be caused by man-made via factories and glass waste. Fires cause great damage to the environment and may lead to human death. Unfortunately, the fire that broke out in AL-Qoubaiyat and Tyre in Lebanon, have been witnessed and caused great damage to the environment, human losses, etc. In this study, a study of fire risk management for those two study areas, will be analyzed using two types of data (Landsat-8 and Sentinel-2) for AL-Qoubaiyat case study, whereas it will be between (Landsat-7 and Sentinel-2) for the Tyre case study. The Analysis will be done by using the Normalized Burn Ration (NBR), Differenced Normalized Burn Ration (Δ NBR) along with all type of required atmospheric corrections. According to our study, it was found advisable to monitor fire risk management using Sentinel-2 L2A data since the atmospheric correction is already performed on it but for L1C data the Sen2Cor python must be used to apply atmospheric correction. Furthermore, the Sentinel-2 L2A data analysis gave more precise results than Landsat-8 by about 2% in Sour case study and 5.7 % in AL-Qoubaiyat case study. Hoping that this method will help in tracking fires, disaster risk reduction, and help in classifying burn severity accompanied with calculating the area corresponding to each class.

1. INTRODUCTION

Since ancient times, forests have been considered an integral part of the human ecosystem and its environment. Frankly, they are the greatest bounty of nature to mankind and play a very important role in its life. In addition to providing shelter and protection to a great number of living beings, including pre-historic man, forests have been the main source of food, wood, and a large variety of other products. In fact, forests have played an important role in various economic, social, and religious activities in human life. Globally, forests encounter increasing challenges and risks from natural disasters, which continue to strike unabated without warning and are consistently increasing in their magnitude, frequency, complexity, and economic impact. To clarify, a forest fire is the most common hazard in forests as well as it is one of the

major disasters responsible for forests' degradation. In fact, forest fires have multiple causes as well as many consequences.

Those forest fires are caused either by anthropological or natural causes. In general, all over the globe, the majority of fires are caused by human activity (Ali, 2020). According to estimation, there are about 50,000 fires that occur each year in the Mediterranean basin and affect more than 600,000 hectares. Moreover, a reported number of 251 fires took place in the year 2020 in Lebanon with burnt area equals to 1851 ha. To be clear, the majority cause of fires in the Mediterranean basin is of human origin resulting either by accident, negligence, or intention (Haddad et al., 2014).

There are many consequences of forest fires, besides posing a serious threat to the forest's wealth, it also affects the entire regime of flora and fauna, thus disturbing the biodiversity of ecology and

* Corresponding Author

(mohamed.issa@liu.edu.lb) ORCID ID 0000-0002-8263-2225
(mohammad.abboud@liu.edu.lb) ORCID ID 0000-0003-3810-633X

Cite this article

Issa, M., & Abboud, M. (2022) Forest fire disaster risk analysis using Sentinel 2 and Landsat images case study: Al-Qoubaiyat and Tyre regions, Lebanon. Turkish Journal of Geosciences 3(2), 84-94.

environment. However, the impact of forest fires is not limited only to its physical component but also goes beyond it as it affects the socio-economic condition of the affected population. Moreover, forest fires also can have global consequences as it produces gaseous and particle emissions that affect the composition and functioning of the jet stream and the global atmosphere, exacerbating climate change as they feedback in global warming since they result from burning vegetation and release of stored carbon (Ali, 2020).

During the last decades, many researchers tried to analyze the usage of Remote Sensing (RS) techniques for forest fire risks, prevention, assessment and monitoring. These techniques have been employed to address three different temporal fire-effects phases: pre-fire conditions, active fire characteristics and post-fire ecosystem responses (Chu and Guo, 2014). Numerous algorithms and approaches for the first two phases have been developed; little effort, however, has yet been dedicated to assessing suitable RS data and methods over the widely spatial and temporal ranges of post-fire-affected environments.

Within the fire science community, there are a variety of terms used to describe the characteristics of fire and its effects. For instance, Sabuncu and Ozener, (2018), reviewed some of these terms: pre-fire environment, fire environment, active fire, post-fire environment, fire regimes defined by fire intensity, fire and burn severity, season of burn, type of fire and burned size and shape. They addressed many factors that can be used to detect fire severity and analyze its effect. Some of these factors are: NBR, Δ NBR, NDVI, Δ NDVI, pixel based classification, and object based classification (Sabuncu and Ozener, 2018). On the other hand, different RS data sources can be used related to a forest fire analysis. Fire-damaged areas could be identified by classifying optical satellite images such as Landsat or MODIS. Object-based classification and spectral classification are some of these methods. In addition, calculating land surface temperature with thermal bands of optical images is used to determine fire areas. Besides, topographic parameters such as elevation, slope, and aspect could be produced from the Shuttle Radar Topographic Mission (SRTM) in order to determine fire risk severity. Topographic factors can be integrated into a geographic information system and these areas can be determined by giving certain weights to them. Also, spectral fire indices are used to identify forest fire zones and risk areas (Navarro et al., 2017).

After looking generally at the causes and consequences of fires in forests, this study will focus mainly on Lebanon and specifically in Al-Qoubaiyat and Tyre regions. Since Lebanon has recently witnessed many fires in its forests that not only affected the plant and animal wealth but also

threatened the lives of the citizens with death. The fires occurred in 2021 and caused a great damage.

Because of this, we have used two sources of RS data, that are Sentinel-2 and Landsat (8 and 7) images (pre-fire and post-fire, Table 2 and Figure 5) to evaluate the burnt area in AL-Qoubaiyat and Sour regions corresponding to fires produced during July 2021. Those studies could help us understand both the causes and consequences of spatial variability of post-fire effects. Therefore, the main aim of our study was to test the suitability of Sentinel-2 MSI data and Landsat Operational Land Imager (OLI) for mapping different spectral indices related to the burn severity of the Al-Qoubaiyat and Tyre fires. These indices are cost-effective and spatially comprehensive views of both areas that have been affected by fire in different fire grading.

The Analysis will be oriented toward the selection of best suitable data for fire forest management, used parameters for classification, required corrections, and results analysis. Therefore, in order to accomplish the mentioned aims, the Landsat 8, Landsat 7, and Sentinel 2 data images will be used. In addition, NBR and Δ NBR indices will be used to create the fire risk classes.

2. METHOD

2.1. Study Area

2.1.1. Al-Qoubaiyat area

Al-Qoubaiyat is a village located in the northeast of the Lebanese republic spreading along 70 square kilometers almost and with an elevation of 700 meters above sea level. It is limited by "Akkar al-Atika" village to the west, and by the line that separates the two districts of Akkar (North) and the Hermel "Bekaa" to the east. Al-Qoubaiyat population is mostly around 12,000 persons. It is usually full of people during the summer but few of them stay during the winter due to the severe coldness of the area and the snow. This area suffers from frequent multiple fires every year. Figure 1 illustrates the location of Al-Qoubaiyat study area.

On the 28th of July in 2021, the region of Al-Qoubaiyat, the most greeny scurb and forests area of Akkar, turned into burned area after her core was burnt as a result of successive fires that broke out in it. Briefly, these fires left great destruction in the green forested areas and pine forests; as well it threatens the lives of the residents along with the forest. But the cause of the fire remains unknown, as it is expected to be due to glass waste and human neglect. The cause of the fire spread on such a large scale refers to the wind, dry vegetation, and the overcrowding of the area with forest trees.

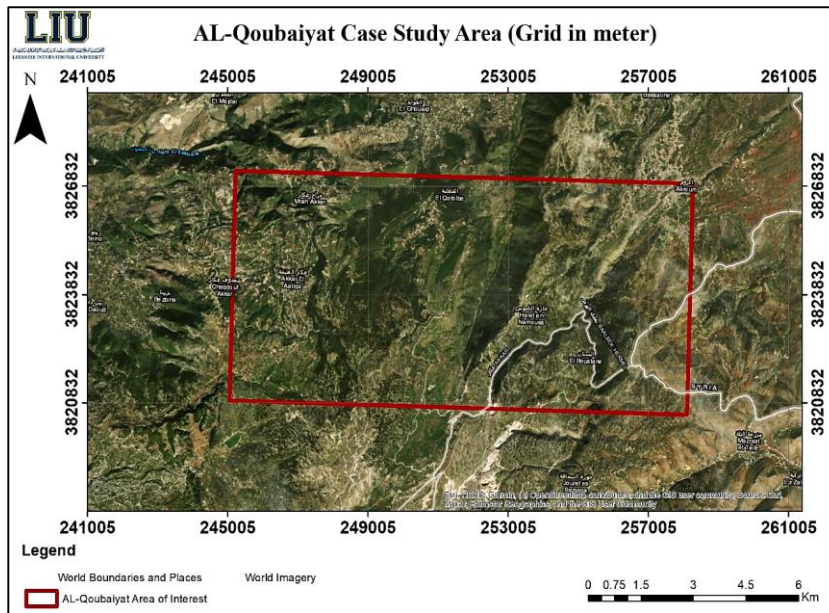


Figure 1. Al-Qoubaiyat study area

2.1.2. Sour (Tyre) Area

The city of Tyre (sour) is situated along the Mediterranean coast, around 80 kilometers south of Beirut with an area of 5 square kilometers. The city is one of the best tourist cities in Lebanon and includes many archaeological sites, which attracts tourists to visit it. Figure 2 illustrate the location of Sour study area. Unfortunately, on November 13,

2021, a huge fire broke out in Wadi AL-Aziya-Zebin in the Tyre region and it spread over large areas of agriculture and forest. The strong winds contributed to the approach of the fire to the residential houses in the town of Haniyeh, Zebin, and Majdel-Zone. The leadership of the Lebanese army suggested that the fire was made by unknowns and spreads through due to the presence of wind, leading to that big damage.

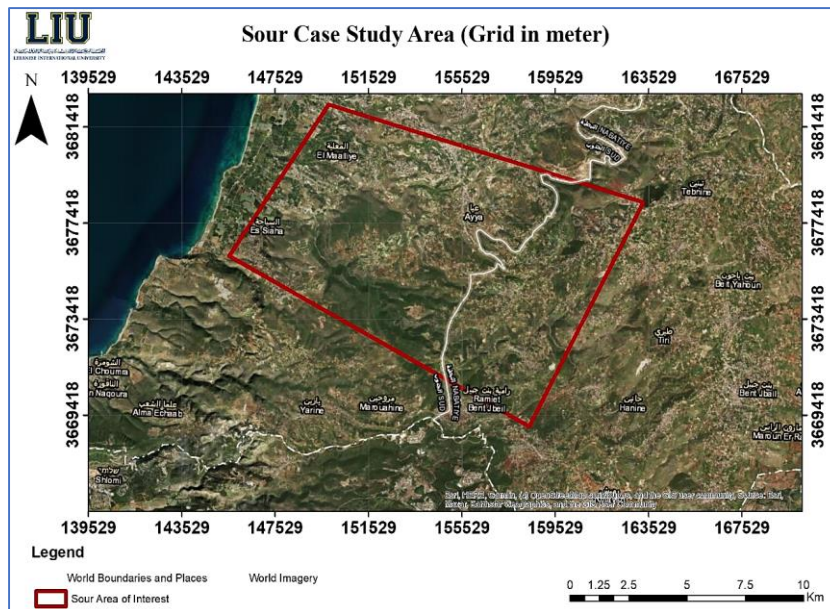


Figure 2. Sour study area

2.2. Methodology and Materials

The methodology demonstrates the procedure that was followed to choose, process, and analyze the data. Fire monitoring is an important project in which it gives information about the burned area,

classification and how to deal with its spread day by day basis. The same methodology was adopted for the two case study areas, that are Al-Qoubaiyat and Tyre in Sour regions. Below, flow chart that represents the methodology that was adopted in this study (Figure 3).

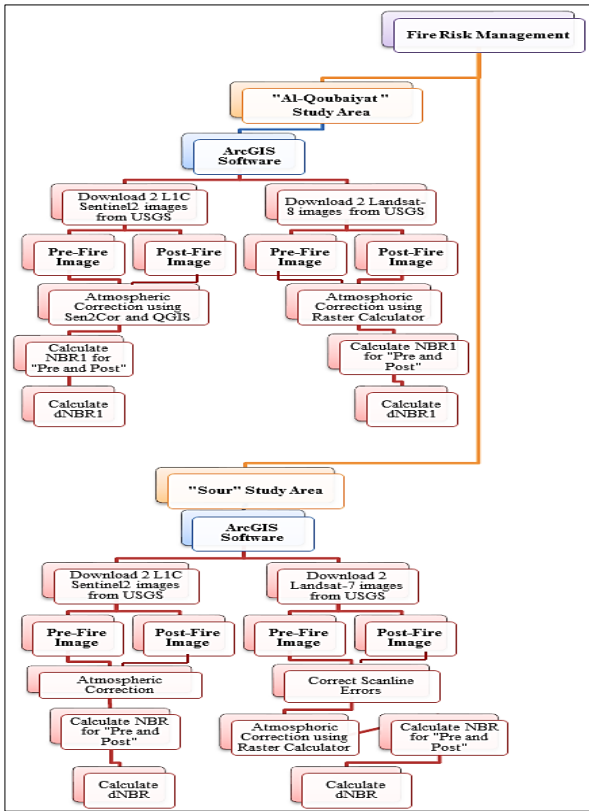


Figure 3. Flowchart illustrating the adopted methodology

The adopted methodologies used in this study, and illustrated in the previous flowchart, are explained briefly as follows:

Processing of Sentinel 2 L1C data:

- Use sen2cor python and QGIS Semi-Automatic Classification Plugin methods to correct the effects that the atmosphere has on Sentinel-2 L1C image data and to obtain the L2A surface reflectance product.
- Import the corrected Sentinel 2 bands (8a, 4, 12) (NIR, Red, SWIR2) to the ArcGIS.
- Then, divide each band by 10,000 using the raster calculator tool.
- After masking water bodies for all bands, use the raster calculator to calculate the (NBR) and (Δ NBR) for both pre and post-fire data of Sentinel.
- Classify the values using burn severity classification and use the reclassify command from the spatial analyst tool to give each class a value.
- Open the attribute table of the reclassified Δ NBR and calculate each burned area.
- Use the conversion tools to transform the reclassified Δ NBR data to a polygon.

Processing of Landsat data:

- Correct Scanline errors for each band used (4, 7) (NIR, SWIR2) in Landsat-7 data by using "fix Landsat 7 Scanline Errors" tool.
- Using the raster calculator tool in ArcGIS, apply an atmospheric and sun angle

correction for Landsat-8 bands (7, 5, 4) (SWIR2, NIR, Red) and Landsat-7 bands.

- Import the corrected Landsat-8 bands (7, 5, 4) (SWIR2, NIR, Red) and the corrected Landsat-7 bands to the ArcGIS.
- Create a polygon shapefile for Landsat data to digitize water bodies.
- Then, use image analysis to mask water bodies using the digitized shapefiles.
- Calculate the (NBR) and (Δ NBR) for both pre and post-fire data of Landsat-8.
- Classify the values using burn severity classification and using reclassify command from spatial analyst tool to give each class a value.
- Open the attribute table of the reclassified Δ NBR and calculate the area.
- Use the conversion tools to transform the reclassified Δ NBR data to a polygon

2.2.1. Software used

A Geographic Information System is a system of computer software that allows the user to enter, manipulate, analyze, and display information that is related to a certain location on the earth's surface. Since forest fires are considered one of the major causes of natural resource destruction, and this is often watched on a global scale, RS and GIS technologies are valuable disciplines in studying the features of the land in which they help in monitoring and detecting the forest fires' causes. In addition, GIS also helps in understanding how to decrease the impacts of forest fires and find a solution to various issues related to it. For instance, GIS software can play an important role before the fire by which it helps the municipalities to mark the exact locations of fire hydrants **Hata! Başvuru kaynağı bulunamadı.** (Stone, 2016). Moreover, GIS can serve an important function in terms of monitoring the burned areas resulting from forest fires and estimating their surface areas.

• Importance of the Use of QGIS in Monitoring Fires:

Concerning the QGIS, it is an acronym for Quantum Geographic Information System which is computer software that allows its users to edit, view, check, and process geospatial data. Moreover, it allows assessing and editing the spatial information needed and creating new maps. In addition, QGIS has many tools functions and it is considered very fast compared to other applications.

QGIS can serve as an important role in monitoring the burned areas resulting from forest fires. Through the QGIS tools, the user can analyze and determine the area affected by fire and classify its burn severity. QGIS tools allow users to employ satellite-based imagery and derivative information to produce a burn severity map and to provide an

important additional resource that supports fire managers.

- **Importance of the Use of Sen2Cor python in Atmospheric Correction:**

Sen2Cor is a prototype processor used to perform a pre-processing of Sentinel-2 Level-1C (L1C) Top of Atmosphere (TOA) image data where it applies an atmospheric correction and converts into Level-2A Bottom of Atmosphere (BOA) reflectance product. To add, it is used for Sentinel-2 data for land applications to ensure the highest quality of scientific exploitation (Mueller-Wilm et al., 2017).

2.2.2 Parameters used in forest fire analysis

NBR and ΔNBR were used as spectral indices for forest fires burn severity monitoring and analysis. The Normalized Burn Ratio “NBR” is an index designed to highlight areas burned in huge fire zones. Its equation is similar to NDVI, except that the equation combines the utilization of both Near Infrared (NIR) and Shortwave Infrared (SWIR) wavelengths as shown in Figure 4.

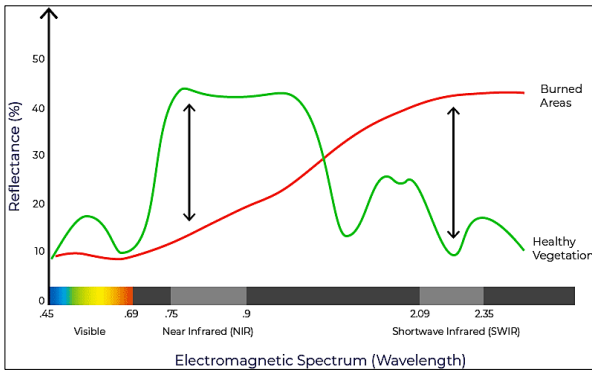


Figure 4. Comparison of the spectral response of healthy vegetation and burned areas (Keeley, 2009)

As shown in Figure 4, healthy vegetation represents a very high reflectance in the NIR portion and a low reflectance in the SWIR portion of the electromagnetic spectrum. This is in contrast to what is seen in areas devastated by fire; recently burnt areas show low reflectance in the NIR portion and high reflectance in the SWIR portion. Accordingly, the difference between the spectral responses of burnt areas and healthy vegetation reach their apex in the NIR and the SWIR portions of the electromagnetic spectrum.

The formula of NBR uses the ratio between NIR and SWIR bands but for making it more accurate some modification in the index was done which is shown in equation number 1. To clarify, a high NBR value signifies healthy vegetation however a low NBR value signifies bare ground and recently burnt areas. The non-burnt areas are normally attributed to values near zero (Keeley, 2009). The following

equation (equation number 1) shows the formula used to calculate the NBR value (Ryu et al., 2018).

$$NBR = \frac{NIR - SWIR}{NIR + SWIR} \quad (1)$$

Where:

NIR: Near Infrared Value

SWIR: Shortwave Infrared wavelengths

Moreover, the burn severity can be estimated from the delta NBR (dNBR or ΔNBR) which can be calculated from the difference between the pre-fire and post-fire NBR obtained from the images (Walz, et al., 2007). The equation below illustrates how to calculate dNBR (equation 2).

$$\Delta NBR = Prefire\ NBR - Postfire\ NBR \quad (2)$$

Furthermore, a classification table to interpret the burn severity was proposed by the United States Geological Survey (USGS) which can be seen in the table below (Table 1). The burn severity data and maps can help in developing emergency rehabilitation and restoration plan after the fire. In addition, they can be utilized to estimate not only the soil burn severity, but also the probability of future downstream impacts due to flooding, soil erosion, and landslides (Keeley, 2009).

Table 1. The Burn Severity levels, proposed by USGS (Rozario et al., 2018)

ΔNBR	Burn Severity
< -0.25	High post-fire regrowth
-0.25 to -0.1	Low post-fire regrowth
-0.1 to +0.1	Unburned
0.1 to 0.27	Low-severity burn
0.27 to 0.44	Moderate-Low-severity burn
0.44 to 0.66	Moderate High-severity burn
> 0.66	High-severity burn

2.3. Data Collection and Acquisition

In this study the results obtained from two different sources, namely: The Landsat 8 and the Sentinel 2 satellite images for Al-Qoubaiyat study area before and after fire occurrence, were analyzed. The following Table 2 illustrates the differences between the two data sources. On the other hand, for Tyre in Sour region, this case study used the images from Landsat-7 Enhanced Thematic Mapper + (ETM+) and Sentinel 2 satellite images. The main differences between Landsat-7 and Landsat-8 sensors are not only in the numbers of the spectral ranges but also in the radiometric resolution, which is 16 bits for the Landsat 8 OLI platform, and 8-bits

for the Landsat-7 ETM + (Figure 5). The fact that different sensors with different spectral and radiometric resolution are used for change detection

process should be taken into account during the results analysis.

Table 2. Illustration of the differences between Sentinel 2 and Landsat 8 data (Korhonen et al., 2017)

Sentinel-2			Landsat 8		
Band Specification	Wavelength (nm)	Resolution (m)	Band Specification	Wavelength (nm)	Resolution (m)
Band 1—Coastal	433-453	60	Band 1—Coastal	433-453	30
Band 2—Blue	458-523	10	Band 2—Blue	450-515	30
Band 3—Green	543-578	10	Band 3—Green	525-600	30
Band 4—Red	650-680	10	Band 4—Red	630-680	30
Band 5—Vegetation red edge	698-713	20	Band 5—NIR	845-885	30
Band 6—Vegetation red edge	734-748	20	Band 6—SWIR	1560-1660	30
Band 7—Vegetation red edge	765-785	20	Band 7—SWIR	2100-2300	30
Band 8—NIR	785-900	10	Band 8—Panchromatic	500-680	15
Band 8a—Vegetation red edge	855-875	20	Band 9—Cirrus	1360-1390	30
Band 9—Water vapor	930-950	60	Band 10—Thermal	10,600-11,200	100
Band 10—SWIR—Cirrus	1365-1385	60	Band 11—Thermal	11,500-12,500	100
Band 11—SWIR	1565-1655	20			
Band 12—SWIR	2100-2280	20			

Landsat 7 ETM+ Bands (mm)	Band 1	30 m Blue	0.441 - 0.514
	Band 2	30 m Green	0.519 - 0.601
	Band 3	30 m Red	0.631 - 0.692
	Band 4	30 m NIR	0.772 - 0.898
	Band 5	30 m SWIR-1	1.547 - 1.749
	Band 6	60 m TIR-1	10.31 - 12.36
	Band 7	30 m SWIR-2	2.064 - 2.345
Landsat 8 OLI and TIRS Bands (mm)	Band 8	15 m Pan	0.515 - 0.896
	Band 1	30 m Coastal/Aeros	0.435 - 0.451
	Band 2	30 m Blue	0.452 - 0.512
	Band 3	30 m Green	0.533 - 0.590
	Band 4	30 m Red	0.636 - 0.673
	Band 5	30 m NIR	0.851 - 0.879
	Band 6	30 m SWIR-1	1.566 - 1.651
	Band 7	30 m SWIR-2	2.107 - 2.294
	Band 8	15 m Pan	0.503 - 0.676
	Band 9	30 m Cirrus	1.363 - 1.384
	Band 10	100 m TIR-1	10.60 - 11.19
Band 11	100 m TIR-2	11.50 - 12.51	

Figure 5. Illustration of the differences between Landsat 7 ETM and Landsat 8 data (Jovanović et al., 2015)

The satellites images used within the scope of this study were obtained free of charge from the United States Geological Survey (USGS) site in UTM projection. The gathered data are:

- For El_Qoubaiyat study area:
 - Sentinel 2 satellite data from USGS for Qoubaiyat: pre-fire (19/7/2021) and post-fire (3/8/2021).
 - Landsat 8 satellite data from USGS for Qoubaiyat: pre-fire (26/7/2021) and post-fire (11/8/2021).

During this stage, the collected data are processed using ArcGIS. To clarify, Sen2Cor python is used only to apply an atmospheric correction for L1C Sentinel 2 data.

- For Sour study area:
 - Sentinel-2 satellite data from USGS for Sour: pre-fire (11/11/2021) and post-fire (16/11/2021).ss

Landsat-7 satellite data from USGS for Sour: pre-fire (7/11/2021) and post-fire (23/11/2021).

2.3.1. Notes on data processing:

In order to obtain the burned areas from the gathered data, the following processing corrections were made:

- The sen2cor python was used to correct the effects that the atmosphere has on Sentinel-2 L1C image data and to obtain the L2A surface reflectance product.
- The ArcGIS image analysis was used to mask water bodies using the digitized shapefiles. This due to that ΔNBR is sensitive to water and thus, sometimes pixels that are classified as high severity may be water (Rutkay et al., 2020).
- The symbology and reclassify command were used to classify the values using burn severity classification according to the classification Table 1.
- The ArcGIS raster calculator tool was used to apply an atmospheric and sun angle correction for Landsat-8 bands (7, 5, 4) (SWIR2, NIR, Red).
- Correct Scanline errors for each band used (4, 7) (NIR, SWIR2) in Landsat-7 data by using “fix Landsat 7 Scanline Errors” tool. That is, “fix Landsat 7 Scanline Errors” tool which found in the Landsat Toolbox was first used in order to correct the Scanline errors for each band used. After that, equation (3) was applied for each band by using the raster calculator tool and with the aid of information found in the metadata file of the Landsat-7.

$$(TOA\ reflectance = \frac{Band \times (Radiance_Max_Band - 255 - Radiance_Min_Band + 255) - Radiance_Min_Band}{\sin(\text{sun elevation})}) \quad (3)$$

3. RESULTS

After calculating NBR for pre and post-fire of both Sentinel-2 and Landsat-8 data, the indices Δ NBR were calculated using the raster calculator tool and in reference to equation No. 1 and 2. As a remark, setting an analysis mask for these indices must be done before processing where Δ NBR indices were masked according to a previously digitized shapefile for burned area. To clarify, this step that was done in the environment tab means that the processing for Δ NBR will only occur on locations that fall within the mask.

Concerning the classification of burn severity, it was done inside the ArcGIS using properties of calculated Δ NBR layer (Symbology) and in accordance to Table 1.

Area calculation for burn severity classes was done using the reclassification tool and multiplying the count number in each class by the cell size, taking into account that the cell size of sentinel-2 image is (20×20) m while that of landsat-8 is (30×30) m. After that, the L2A and Landsat-8 data of burned areas were arranged in excel, and the difference in area between them was calculated. For the 4 individual polygons that represent burned areas, the percentage of area difference between L2A and Landsat-8 data was calculated by dividing their area difference by the polygon area for L2A data since total L2A area is more than total Landsat-8 area. Afterwards, the percentage for the total difference was calculated by dividing the total difference value by the total L2A area (see Table 3 and Figure 6).

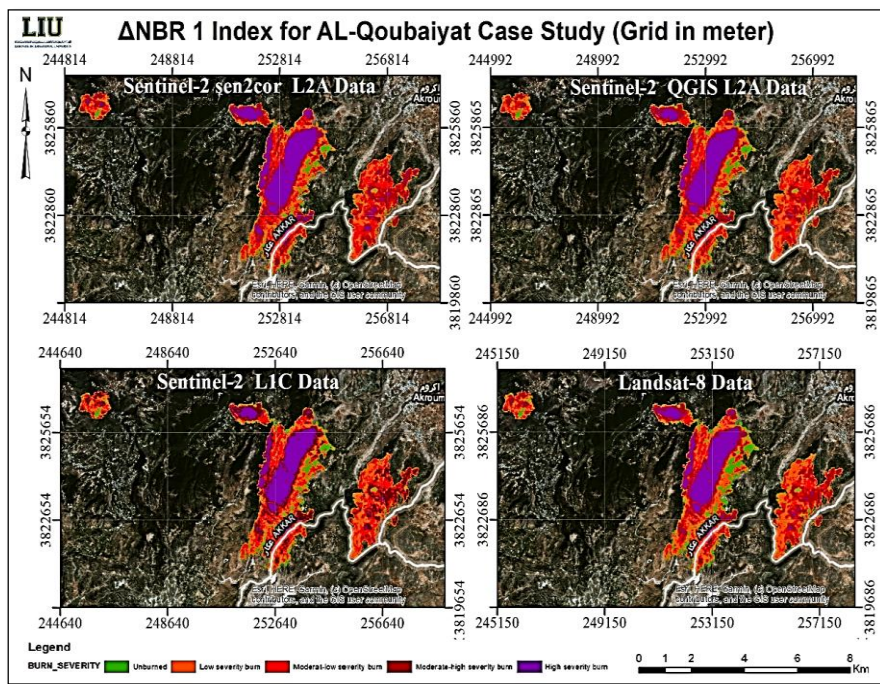


Figure 6. The dNBR classified map for Al-Qoubaiyat case study

Table 3. Table includes percentage of area difference between L2A and Landsat-8 Data for Al-Qoubaiyat area polygons

Al-Qoubaiyat	Polygon Area (Km ²)	(L2A-Landsat 8) km ²	Percentage of area difference between L2A and Landsat-8 data
Burned Area 1	0.721	0.035	4.9 %
Burned Area 2	0.848	0.031	3.6 %
Burned Area 3	4.035	0.118	2.9 %
Burned Area 4	8.632	0.630	7.3 %
Total Area	14.235	0.814	5.7 %

From this table, it can be seen that either Sentinel-2 or Landsat images can be used to classify and estimate the fire risks with difference ranges between 3 % to about 7 %. In addition, since the areas were arranged in ascending manner, this difference is increased as the area of spotted polygon increased. The difference may be attributed also to

the difference in pixel size between the two data sources. The calculated area was compared to the values estimated by the CNRS and they were very close and the differences can be attributed to the fact that CNRS had used a different post-fire image data from ours where the fires that had ignited post 29 July were not considered in the statistics of CNRS

map. For instance, (as depicted in Figure 7.), the reported burned area from CNRS was 10.27 km², the moderate to low severity was 2.71 km², the moderate to high severity was 3.85 km², and the high severity was 3.72 km².

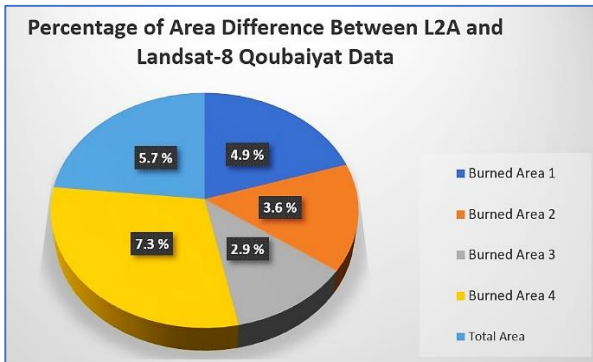


Figure 7. Illustration of the difference in area calculation for burned areas between L2A and Landsat-8

Figure 8 represents two classified fire burn severity maps for Al-Qoubaiyat case study; one resulted from Sentinel-2 L1C data atmospherically corrected using Sen2Cor python and second resulted from atmospherically corrected Landsat-8 data. These two results that obtained from Sentinel-2 Sen2Cor L2A and Landsat-8 data are similar visually with some differences in unburned, low-severity burn, and Moderate-low severity burn classes in the east side of the biggest burned area limit which may be due to the cell size difference between these two data images. Moreover, in the smallest polygon to the left the high severity class differs between L2A and Landsat-8 where it is wider in L2A than in Landsat-8. On the other hand, the high severity area almost equals to the low severity area where both of them equals to about 3.45 km². It should be noted that every year the fire took place in this region, and as can be seen, it starts in four different places which makes someone believes that fires were due to arson.

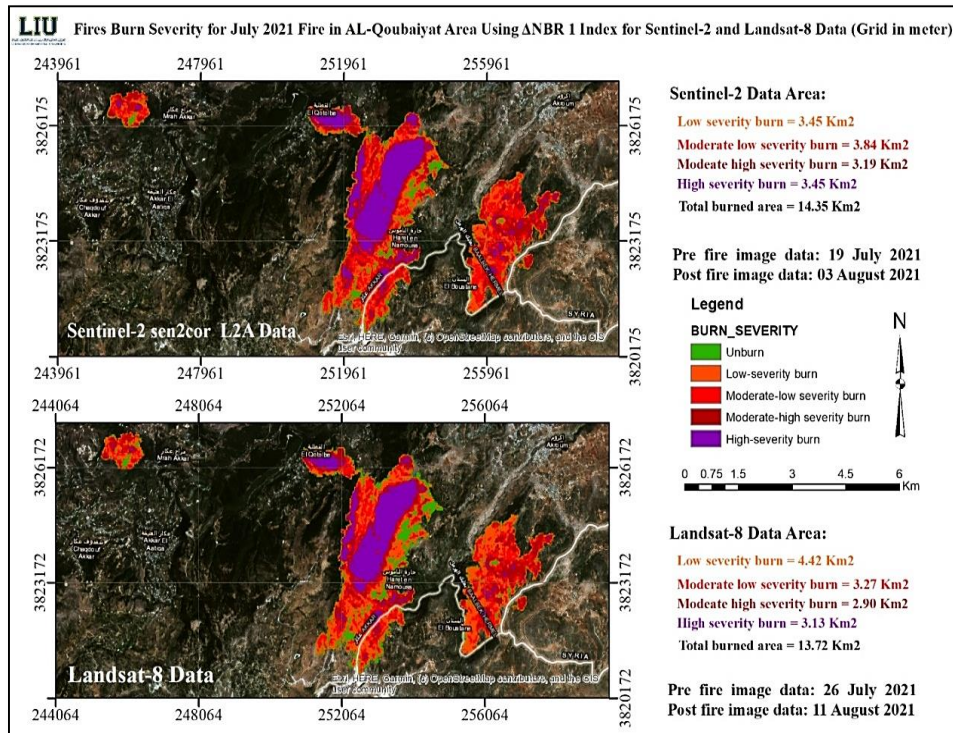


Figure 8. Figure showing fire burn severity map for July 2021 fire in Al-Qoubaiyat area using dNBR index for Sentinel-2 L2A data and Landsat-8 data

Concerning the Sour case study, the resulted fire burn severity maps for November 2021 fire using dNBR index, as calculated from Landsat-7 images, are shown in the Figure 9. These maps are also classified according to burning severity levels into 5 classes noting that data was also atmospherically corrected. From this figure, it can be seen that the

burn severity classification in this figure is logical visually where the moderate low severity burn class is dominant, the high severity class is present at the center of fire, and the unburned class is present at the border of the burned area and this corresponds to the actual fires noticed on the ground by fire fighter's groups shared in extinguishing fires.

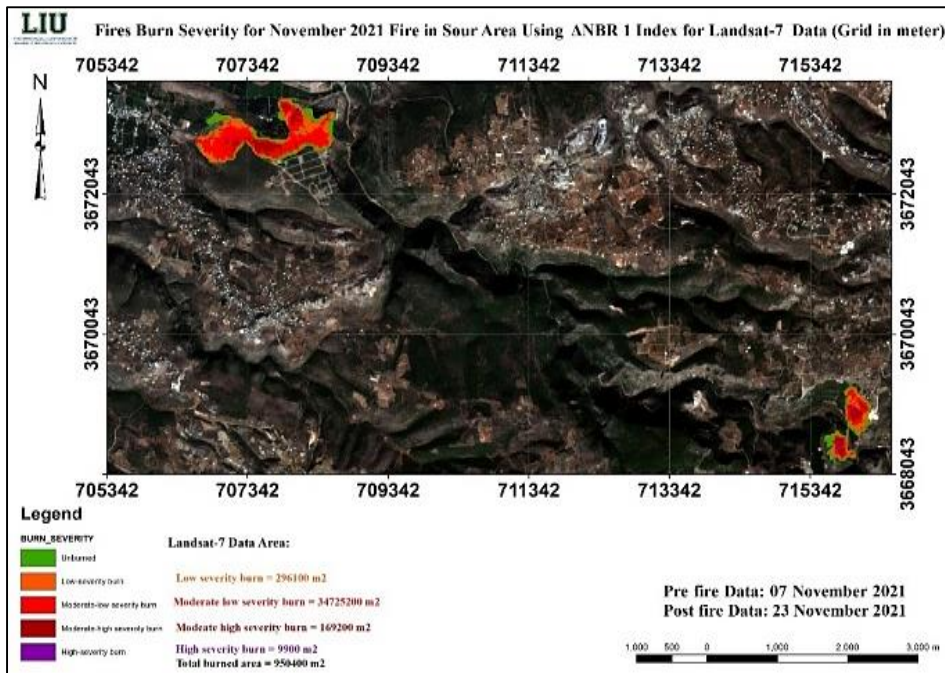


Figure 9. Illustration of fire burn severity map for November 2021 in Sour area using dNBR index for Landsat-7 data

Concerning the Sentinel-2 data, for Sour city, Figure 10. shows a classified map that is resulted from Sentinel-2 L1C data atmospherically corrected using Sen2Cor python. In this figure, it is noticeable that the low severity class is the dominant class, the high severity class is present at the center of fire, and the unburned class is also present at the border of

the burned areas. In addition, as written on the map, the low risk area equals to 100,1200 m², the moderate low severity equals to 406,800 m², the moderate high severity equals to 406,800 m², the high severity equals to 72,000 m², the total burned area equals to about 180,000 m².

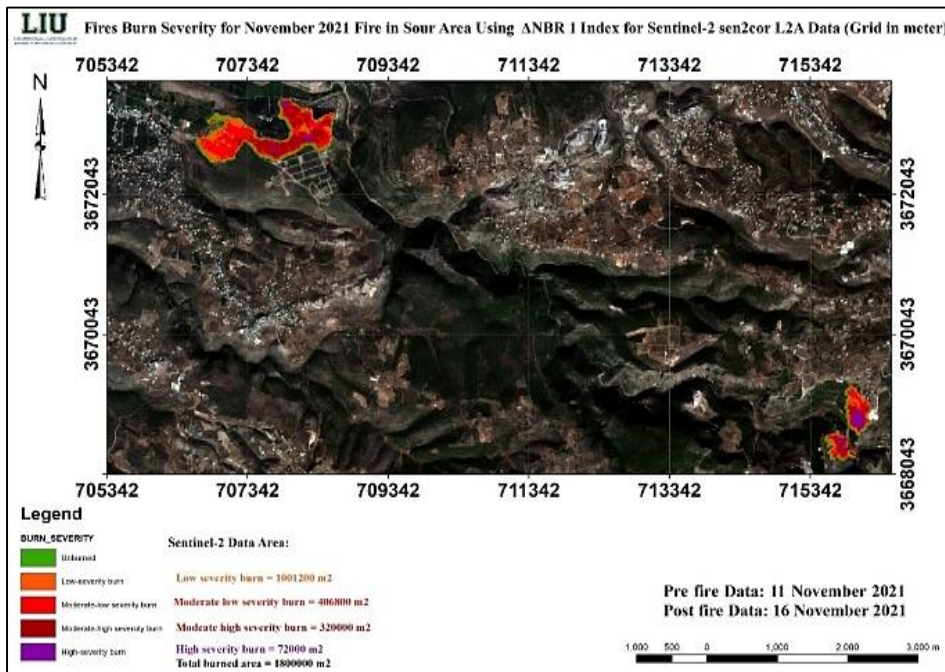


Figure 10. Demonstration of fire burn severity map for November 2021 in Sour area using dNBR index for Sentinel-2 Sen2Cor L2A data

In the following Figure 11, two classified fire burn severity maps for Sour case study are shown. The first one was resulted from Sentinel-2 L1C data

and atmospherically corrected using Sen2Cor python, whereas the second one was resulted from atmospherically corrected Landsat-7 data.

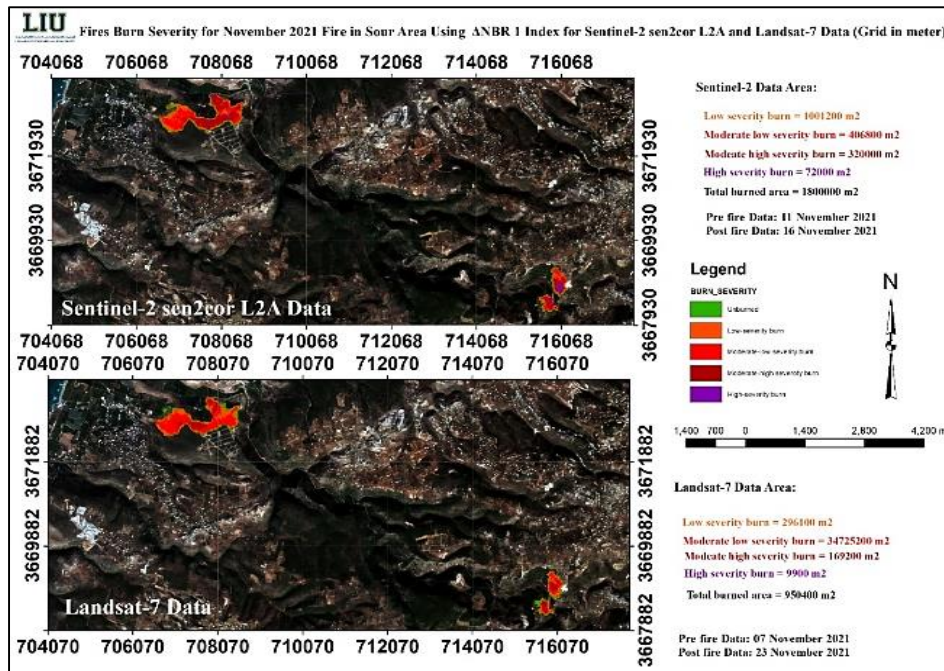


Figure 11. Figure showing fire burn severity map for November 2021 fire in Sour area using dNBR index for Sentinel-2 L2A data and Landsat-7 data

These two results that were obtained from Sentinel-2 Sen2Cor L2A and Landsat-7 data are, also, similar visually with some differences in burn severity classes at the border and at the center of fire region. To explain further, the moderate-high severity burn class at the center of fire region is higher in Sentinel-2 Sen2Cor L2A data than that in Landsat-7 data. That is, the unburned class in Landsat-7 is more noticeable than in Sentinel-2 L2A at the borders.

The following Table 4 represents the percentage of area difference between Sentinel-2 L2A and Landsat-7 data for the 2 biggest polygons in Sour case study. The area values in this table were calculated with the use of polygons area in ArcMap. It can be noticed that the percentage of the total area difference between Sentinel-2 L2A and Landsat-7 burned area is 2% which differs from that in Al-Qoubaiyat case study “5.7%”.

Table 4. The percentage of area difference between L2A and Landsat-7 Data for the 2 biggest polygons “Sour”

Sour Case Study	Shape Area L2A (m ²)	Shape Area Landsat 7 (m ²)	Area Difference (L2A-Landsat 7) m ²	Percentage of area difference between L2A and Landsat-7 data
Burned Area 1	747766.264	740979.556	6786.7082	0.9 %
Burned Area 2	151185.038	138117.578	13067.4608	9.4 %
Total Area	898952	898952	19854.169	2 %

From the previous table, it can be noticed also that the difference is increased as the area of spotted polygon increased.

4. CONCLUSIONS AND RECOMMENDATIONS

In conclusion, through this study two types of data for each of Al-Qoubaiyat and Sour case studies were handled. In addition, multiple atmospheric correction methods were applied in a way to verify the most reliable data. The data used for Al-Qoubaiyat case study are the Sentinel-2 L1C data and the Landsat-8 data while for Sour case study are the Sentinel-2 L1C data and the Landsat-7 data. A categorized map for both case studies showing the severity of burns as well as the area values for each

category, were obtained. According to performed analysis, among the atmospheric correction methods for Sentinel-2 L1C data, the most reliable and accurate correction method is Sen2Cor python. According to the work that was done and clarified previously about the “5.7%” between Sentinel-2 L2A and Landsat-8 data in Al-Qoubaiyat, it can be said that Sentinel-2 data is the most reliable data that can be directly relied upon in fire risk management due to its cell size and its complete full earth coverage each 10 days. To be clear, Sour case study came to verify the results that were obtained in Al-Qoubaiyat where the analysis also gave a positive value “2%” meaning that Sentinel-2 still gave more burnt area than Landsat.

Therefore, henceforth, for any fire or fire spark that may occur in the future, anyone who wants to study and monitor fire risk management he can directly use Sentinel-2 L2A data since the atmospheric correction is already performed on it but for L1C data the Sen2Cor python must be used to apply atmospheric correction.

According to study findings, it is recommended:

If possible, use post-fire image data as close as possible to the date of fire disaster to avoid the regrowth of burned vegetation.

Directly use Sentinel-2 L2A data or L1C data atmospherically corrected using Sen2Cor python.

Make sure to mask water bodies, if existed in your case study, before calculating NBR index in order to ensure that these bodies will not affect this index.

In addition, it is recommended for future work to categorize the trees in the vegetation texture according to their types to increase the accuracy of the study.

Using QGIS is much easier over traditional ArcGIS since for automatic correction of data atmospherically.

Acknowledgement

We are also grateful to the three anonymous reviewers for their constructive comments.

Author Contributions

Mohamed Issa: Conceptualization, Methodology, Software and Data curation. **Mohammad Abboud:** Data download and editing, Writing- Original draft preparation and contributed to the discussion.

Conflicts of Interest

The authors declare no conflict of interest.

REFERENCES

Ali, E. (2020). Geographic Information System (GIS): Definition, Development, Applications & Components. *Department of Geography, Ananda Chandra College, India.*

Rutkay, A., Kalkan, K., & Gürsoy, Ö. (2020). Determining the forest fire risk with sentinel 2 images. *Turkish Journal of Geosciences*, 1(1), 22-26.

Haddad, E.A., Farajalla, N., Camargo, M., Lopes, R.L., & Vieira, F.V. (2014). Climate change in Lebanon: Higher-order regional impacts from agriculture. *Region*, 1(1), 9-24.

Chu, T., & Guo, X. (2013). Remote sensing techniques in monitoring post-fire effects and patterns of forest recovery in boreal forest regions: A review. *Remote Sensing*, 6(1), 470-520.

Navarro, G., Caballero, I., Silva, G., Parra, P.C., Vázquez, Á., & Caldeira, R. (2017). Evaluation of forest fire on Madeira Island using Sentinel-2A MSI imagery. *International Journal of Applied Earth Observation and Geoinformation*, 58, 97-106.

Ryu, J.H., Han, K.S., Hong, S., Park, N.W., Lee, Y.W., & Cho, J. (2018). Satellite-based evaluation of the post-fire recovery process from the worst forest fire case in South Korea. *Remote Sensing*, 10(6), 918.

Jovanović, D., Govedarica, M., Sabo, F., Bugarinović, Ž., Novović, O., Beker, T., & Lauter, M. (2015). Land cover change detection by using remote sensing: A case study of Zlatibor (Serbia). *Geographica Pannonica*, 19(4), 162-173.

Keeley, J.E. (2009). Fire intensity, fire severity and burn severity: a brief review and suggested usage. *International journal of wildland fire*, 18(1), 116-126.

Korhonen, L., Packalen, P., & Rautiainen, M. (2017). Comparison of Sentinel-2 and Landsat 8 in the estimation of boreal forest canopy cover and leaf area index. *Remote sensing of environment*, 195, 259-274.

Mueller-Wilm, U., Devignot, O., & Pessiot, L. (2016). Sen2Cor configuration and user manual. *Telespazio VEGA Deutschland GmbH: Darmstadt, Germany.*

Rozario, P.F., Madurapperuma, B.D., & Wang, Y. (2018). Remote sensing approach to detect burn severity risk zones in Palo Verde National Park, Costa Rica. *Remote Sensing*, 10(9), 1427.

Sabuncu, A., & Ozener, H. (2018). Evaluating and Comparing NDVI and NBR Indices Performance for Burned Areas in Terms of PBIA and OBIA in Aegean Region Turkey. *FIG Congress, 2018*

Walz, Y., Maier, S.W., Dech, S.W., Conrad, C., & Colditz, R.R. (2007). Classification of burn severity using Moderate Resolution Imaging Spectroradiometer (MODIS): A case study in the jarrah-marri forest of southwest Western Australia. *Journal of Geophysical Research: Biogeosciences*, 112(G2).

